

# Lattice Boltzmann method for inhomogeneous fluids

S.MELCHIONNA<sup>1</sup> and U. MARINI BETTOLO MARCONI<sup>2</sup>

<sup>1</sup> *INFM-SOFT, Dipartimento di Fisica, Università di Roma and Istituto Nazionale di Fisica della Materia, Piazzale A. Moro 2, 00185, Roma, Italy*

<sup>2</sup> *INFM-SOFT, Dipartimento di Fisica, Università di Camerino and Istituto Nazionale di Fisica della Materia, Via Madonna delle Carceri, 62032, Camerino, Italy*

PACS 47.11.-j – Computational methods in fluid dynamics

PACS 47.61.-k – Micro- and nano- scale flow phenomena

PACS 61.20.-p – Structure of liquids

**Abstract.** - We present a lattice-based numerical method to describe the non equilibrium behavior of a simple fluid under non-uniform spatial conditions. The evolution equation for the one-particle phase-space distribution function is derived starting from a microscopic description of the system. It involves a series of approximations which are similar to those employed in theories of inhomogeneous fluids, such as Density Functional theory. Among the merits of the present approach: the possibility to determine the equation of state of the model, the transport coefficients and to provide an efficient method of numerical solution under non-uniform conditions. The algorithm is tested in a particular non equilibrium situation, namely the steady flow of a hard-sphere fluid across a narrow slit. Pronounced non-hydrodynamic oscillations in the density and velocity profiles are found.

**Introduction.** – The behavior of a confined fluid can be different from that of a bulk fluid in many important aspects. First of all the confinement induces density inhomogeneities which may determine a variety of phenomena having no counterpart in bulk systems [1]. The presence of surfaces, not only alters the average equilibrium properties of fluids, but also affects their time-dependent behavior such as diffusion, momentum and energy transport. As a result, a great effort is currently devoted to the understanding of fluid physics at the nanoscale (see [2] and references therein).

In the last thirty years, a massive effort has been devoted to the understanding of system at thermodynamic equilibrium and new techniques have been developed, among these Density Functional theory (DFT) being perhaps the most versatile [3]. On the contrary, we do not have a similar control over the behavior of non equilibrium systems. Dynamical extensions of DFT have been introduced and tested successfully in the case of colloidal suspensions, where the damped character of the dynamics makes the density the only relevant field [4]. Instead, in the case of standard fluids one needs to fully account for the momentum and energy transport. The natural procedure seems therefore to consider the evolution of both positions and momenta of the molecules and to derive an

equation for the phase-space distribution able to convey the structural information about the microscopic nature of the fluid. Such a task can be achieved by using a modified Enskog-Boltzmann approach, which has been proposed by different authors [5–9].

Our present goal is to provide a procedure able to describe simultaneously the discrete nature of fluids and the transport properties at interfaces and in confining geometries. To this purpose, we briefly recall that the Lattice Boltzmann (LB) method represents a very efficient scheme derived from kinetic theory to simulate fluid flows and transport phenomena [10,12]. Being based on the continuum Boltzmann equation, it accounts for a faithful representation of the macroscopic hydrodynamic behavior. The original idea of LB is to model fluid flows by simplified kinetic equations, the Bhatnagar-Gross-Krook (BGK) relaxation operator being a popular choice to simulate the Navier-Stokes evolution at macroscopic level [10,11]. The LB of McNamara and Zanetti [13] averages the microdynamics by solving the kinetic equation of the particle distribution instead of tracking the motion of each particle. Whereas the original formulation was designed to describe lattice gas of particles and the attention was focused on large scale properties, modern versions of the LB aim to incorporate a more realistic behavior of the

fluid. In particular, since the pioneering work of Shan and Chen [14, 15] there has been a large effort to include the effect of microscopic interactions between fluid molecules into the description [6, 7, 9, 16, 17]. Such interactions have been accounted for by considering the intermolecular force field at a particular point in the fluid. This modification is sufficient to describe non-ideal gas behavior such as phase coexistence and phase separation and various surface phenomena, but it is still unsatisfactory since it does not allow for a systematic prediction of the macroscopic properties starting from the microscopic level.

In other approaches, in order to circumvent such a difficulty the collision terms have been dealt with explicitly, but at the price of introducing gradients of the macroscopic fields [6, 7, 9].

Inspired by recent work on inhomogeneous fluids [18, 19], we propose an alternative scheme to evaluate the interaction terms involved in the kinetic equation. As a result, we obtain evolution equations for the distribution function whose structure is very similar to that employed in Density Functional theory, without the explicit evaluation of gradients of macroscopic fields. We believe that the strategy of using coarse-grained quantities instead of gradients of the relevant fields may give a better representation of fluids confined to narrow systems, as we have learned from the study of equilibrium fluids, where gradient expansions usually give poorer results than non-local density functionals.

In addition, the theory allows to compute equilibrium quantities, such as the surface tension, together with accurate estimates of the bulk transport properties.

**Theory.** – In general, the intermolecular potential of a simple fluid can be decomposed into a repulsive, responsible for the microscopic structure at high packing fraction, and an attractive contribution, which plays a major role in determining the thermodynamic properties. However, in the present paper, which serves as to introduce the method, we confine ourselves to discuss a harshly repulsive fluid, the hard sphere system.

The evolution of the phase-space one-particle distribution  $f(\mathbf{r}, \mathbf{v}, t)$  is represented by the following transport equation:

$$\partial_t f(\mathbf{r}, \mathbf{v}, t) + \mathbf{v} \cdot \nabla f(\mathbf{r}, \mathbf{v}, t) + \frac{\mathbf{F}_e(\mathbf{r})}{m} \cdot \nabla_v f(\mathbf{r}, \mathbf{v}, t) = \Omega[f](\mathbf{r}, \mathbf{v}, t) \quad (1)$$

where  $\mathbf{F}_e$  is an external force and  $\Omega[f]$  represents the effect of the interactions among the fluid particles which we describe via the revised Enskog collision operator [20]

$$\begin{aligned} \Omega[f] = & \sigma^{d-1} \int d\mathbf{v}_2 \int d\hat{\boldsymbol{\sigma}} \Theta(\hat{\boldsymbol{\sigma}} \cdot \mathbf{v}_{12}) (\hat{\boldsymbol{\sigma}} \cdot \mathbf{v}_{12}) \times \\ & \{g_2(\mathbf{r}, \mathbf{r} - \boldsymbol{\sigma}, t) f(\mathbf{r}, \mathbf{v}'_1, t) f(\mathbf{r} - \boldsymbol{\sigma}, \mathbf{v}'_2, t) - \\ & g_2(\mathbf{r}, \mathbf{r} + \boldsymbol{\sigma}, t) f(\mathbf{r}, \mathbf{v}_1, t) f(\mathbf{r} + \boldsymbol{\sigma}, \mathbf{v}_2, t)\} \end{aligned} \quad (2)$$

where  $\mathbf{v}'_1$  and  $\mathbf{v}'_2$  are scattered velocities determined from  $\mathbf{v}'_1 = \mathbf{v}_1 - (\hat{\boldsymbol{\sigma}} \cdot \mathbf{v}_{12})\hat{\boldsymbol{\sigma}}$  and  $\mathbf{v}'_2 = \mathbf{v}_2 + (\hat{\boldsymbol{\sigma}} \cdot \mathbf{v}_{12})\hat{\boldsymbol{\sigma}}$ ,  $\sigma$  is the

hard-sphere diameter,  $\hat{\boldsymbol{\sigma}}$  is the unit vector directed from one particle to another, and  $g_2(\mathbf{r}_1, \mathbf{r}_2|n)$  is the positional pair correlation function.

Equation (1), together with (2), represents a nonlinear evolution equation for the one-particle distribution function,  $f(\mathbf{r}, \mathbf{v}, t)$ , and could in principle be solved numerically by brute force, or by considering a suitable truncation of the open hierarchy of equations for the moments of the distribution function. However, since one is chiefly interested in the evolution of the hydrodynamic moments of the distribution function  $n(\mathbf{r}, t) \equiv \int d\mathbf{v} f(\mathbf{r}, \mathbf{v}, t)$ ,  $n(\mathbf{r}, t)\mathbf{u}(\mathbf{r}, t) \equiv \int d\mathbf{v} \mathbf{v} f(\mathbf{r}, \mathbf{v}, t)$  and  $\frac{3}{2}n(\mathbf{r}, t)k_B T(\mathbf{r}, t) \equiv \frac{m}{2} \int d\mathbf{v} (\mathbf{v} - \mathbf{u})^2 f(\mathbf{r}, \mathbf{v}, t)$ , it is possible to further simplify the form of  $\Omega$  without altering the local transfer of momentum and energy. To this purpose, following Dufty, Santos and Brey (DSB) [5], we replace (1) and (2) by a simpler equation, where the complicated interaction between non hydrodynamic modes is approximated via a BGK-like relaxation term  $-\nu_0[f(\mathbf{r}, \mathbf{v}, t) - n(\mathbf{r}, t)\phi_M(\mathbf{v})]$ ,  $\nu_0$  being a phenomenological collision frequency, chosen as to reproduce the kinetic contribution to the viscosity. The DSB equation can be cast in the form:

$$\begin{aligned} \partial_t f(\mathbf{r}, \mathbf{v}, t) + \mathbf{v} \cdot \nabla f(\mathbf{r}, \mathbf{v}, t) + \frac{\mathbf{F}_e(\mathbf{r})}{m} \cdot \nabla_v f(\mathbf{r}, \mathbf{v}, t) = & \\ - \nu_0 [f(\mathbf{r}, \mathbf{v}, t) - n(\mathbf{r}, t)\phi_M(\mathbf{v})] & \\ + m\beta\phi_M(\mathbf{r}, \mathbf{v}, t) \left\{ (\mathbf{v} - \mathbf{u}) \cdot \mathbf{C}^{(1)}(\mathbf{r}, t) \right. & \\ \left. + \left( \frac{m\beta(\mathbf{v} - \mathbf{u})^2}{d} - 1 \right) C^{(2)}(\mathbf{r}, t) \right\} & \quad (3) \end{aligned}$$

where  $\beta = 1/k_B T(\mathbf{r}, t)$  and  $\phi_M(\mathbf{r}, \mathbf{v}, t) = \left[ \frac{m}{2\pi k_B T(\mathbf{r}, t)} \right]^{3/2} \exp\left(-\frac{m(\mathbf{v} - \mathbf{u})^2}{2k_B T(\mathbf{r}, t)}\right)$ . Moreover,

$$C^{(1)}(\mathbf{r}, t) = \int d\mathbf{v} v_\mu \Omega \equiv -\frac{1}{m} \sum_\nu \nabla_\nu P_{\nu\mu}^c(\mathbf{r}, t) \quad (4)$$

where  $P_{\nu\mu}^c$  is the collisional transfer part of the pressure tensor, and

$$\begin{aligned} C^{(2)}(\mathbf{r}, t) = & \frac{1}{2} \int d\mathbf{v} \sum_\nu (v_\nu - u_\nu)^2 \Omega \\ \equiv & -\frac{1}{m} \sum_\nu [\nabla_\nu q_\nu^c(\mathbf{r}, t) + \sum_\mu P_{\nu\mu}^c(\mathbf{r}, t) \nabla_\nu u_\mu(\mathbf{r}, t)] \end{aligned} \quad (5)$$

arises from the collisional contribution to the heat flux,  $\mathbf{q}^c$ .

Equation (3) reproduces the correct form of the hydrodynamic equations, but treats in an approximate fashion, viz. within a relaxation time approximation, the higher velocity moments contributing to  $f(\mathbf{r}, \mathbf{v}, t)$  and associated with kinetic modes [5].

The specific forms of  $\mathbf{C}^{(1)}$  and  $C^{(2)}$  needed to render feasible the method will be given below. Before doing that, we notice that formula (4) establishes a connection between the present method and Density Functional theory. In fact, in the case of vanishing velocity

and temperature gradients, eq. (4) can be expressed with the help of the excess Helmholtz free energy,  $\mathcal{F}_{exc}[n]$ , as  $C^{(1)}(\mathbf{r}, t) = -\frac{1}{m}n(\mathbf{r}, t)\nabla\frac{\delta\mathcal{F}_{exc}[n]}{\delta n(\mathbf{r}, t)}$ . On the other hand, the term  $C^{(2)}(\mathbf{r}, t)$  describes non isothermal processes and has no counterpart within the standard DFT formalism. Under equilibrium conditions, i.e. in the absence of velocity gradients and thermal gradients one can derive the following equation of state with the bulk pressure given by

$$p_{bulk} = \frac{1}{d} \sum_{\nu=1}^d \left[ P_{\nu\nu}^{kin} + P_{\nu\nu}^c \right]_{bulk} = k_B T \left[ n_b + \frac{2\pi}{3} n_b^2 \sigma^3 g_2(\sigma) \right] \quad (6)$$

where we set the kinetic contribution to the pressure tensor  $P_{\nu\mu}^{kin} = m \int d\mathbf{v} (v-u)_\nu (v-u)_\mu f(\mathbf{r}, \mathbf{v}, t)$  to be diagonal and equal to the ideal gas value. In the general non equilibrium case, we consider eq. (3) by taking into account the full contribution to the pressure tensor stemming, e.g., from shearing perturbations.

**Methods and Results.** – We shall solve eq. (3) by means of the lattice Boltzmann method [12] which has the advantage of being very efficient and robust and accommodates in a natural fashion informations about the microscopic model. We restrict our attention to the isothermal situation.

The original LB method can be viewed as a discretization procedure in velocity space of a kinetic equation [6, 21, 22]. We will employ the popular D3Q19 lattice, constituted by a set of 19 populations. The continuous velocity  $\mathbf{v}$  is replaced by a set of discrete velocities  $\mathbf{c}_i$ , with  $i = 0, 18$ , which are vectors which connect neighboring mesh points  $\mathbf{r}$  on a lattice and where the null vector  $\mathbf{c}_0$  accounts for particles at rest. Accordingly, the distribution function is replaced by an array of 19 populations,  $f(\mathbf{r}, \mathbf{v}, t) \rightarrow f_i(\mathbf{r}, t)$ .

The systematic procedure to discretize the kinetic equation is based on expanding the distribution in a finite set of Hermite polynomial  $f(\mathbf{r}, \mathbf{v}, t) = \omega(v) \sum_{l=0}^K \Phi_{\underline{\alpha}}^{(l)}(\mathbf{r}, t) h_{\underline{\alpha}}^{(l)}(\mathbf{v}) / v_T^{2l} 2^l l!$  where  $\omega(v) = (2\pi v_T^2)^{-d/2} e^{-v^2/2v_T^2}$ ,  $v_T = \sqrt{k_B T/m}$  and by considering a Gauss-Hermite quadrature of order  $2G$  to evaluate the integrals of the type

$$\begin{aligned} & \int d\mathbf{v} v^{\alpha_1} \dots v^{\alpha_M} f(\mathbf{r}, \mathbf{v}, t) \\ &= \sum_{i=0}^G w_i c_i^{\alpha_1} \dots c_i^{\alpha_M} f(\mathbf{r}, \mathbf{c}_i, t) / \omega(c_i) \\ &= \sum_{i=0}^G c_i^{\alpha_1} \dots c_i^{\alpha_M} f_i(\mathbf{r}, t) \end{aligned} \quad (7)$$

where  $w_i$  are quadrature weights and  $f_i(\mathbf{r}, t) \equiv w_i f(\mathbf{r}, \mathbf{c}_i, t) / \omega(c_i)$ . Therefore, the kinetic moments are evaluated via

$$\Phi_{\underline{\alpha}}^{(l)}(\mathbf{r}, t) = \sum_{i=0}^K f_i(\mathbf{r}, t) h_{\underline{\alpha}}^{(l)}(\mathbf{c}_i) \quad (8)$$

Analogously, we expand the collision operator on the finite Hermite set,

$$\Omega(\mathbf{r}, \mathbf{v}, t) = \omega(v) \sum_{l=0}^K \frac{1}{v_T^{2l} 2^l l!} C_{\underline{\alpha}}^{(l)}(\mathbf{r}, t) h_{\underline{\alpha}}^{(l)}(\mathbf{v})$$

and evaluate its moments via

$$C_{\underline{\alpha}}^{(l)}(\mathbf{r}, t) = \int d\mathbf{v} \Omega(\mathbf{r}, \mathbf{v}, t) h_{\underline{\alpha}}^{(l)}(\mathbf{v}) \quad (9)$$

The propagation of the populations is achieved via a time discretization to first order and a forward Euler update,

$$f_i(\mathbf{r} + \mathbf{c}_i, t + 1) - f_i(\mathbf{r}, t) = w_i \sum_{l=0}^K \frac{1}{v_T^{2l} l!} C_{\underline{\alpha}}^{(l)}(\mathbf{r}, t) h_{\underline{\alpha}}^{(l)}(\mathbf{c}_i) \quad (10)$$

Concerning the BGK term appearing in eq. (3), standard calculations lead to the following expression for the local equilibrium

$$\begin{aligned} n(\mathbf{r}, t) \Phi_M(\mathbf{c}_i) &= w_i n(\mathbf{r}, t) \left[ 1 + \frac{1}{v_T^2} \sum_{\nu} c_{i\nu} u_{\nu}(\mathbf{r}, t) \right. \\ &\quad \left. + \frac{1}{2v_T^4} \sum_{\nu, \mu} (c_{i\mu} c_{i\nu} - v_T^2 \delta_{\mu\nu}) u_{\nu}(\mathbf{r}, t) u_{\mu}(\mathbf{r}, t) \right] \end{aligned} \quad (11)$$

which is tantamount to a low-Mach ( $O[Ma^3]$ ) expansion.

In order to obtain a practical scheme we have to specify the explicit form of the collisional contributions to the pressure and to the heat flux. This is done by considering the fact that in a hard-sphere fluid, momentum and energy fluxes can be transferred instantaneously even when the velocity distribution function has a Maxwellian form, provided it peaks at the local hydrodynamic velocity with a spread determined by the local temperature. The explicit expression for the collisional contributions then yields  $C_i^{(0)} = 0$ , fulfilling mass conservation, and

$$\begin{aligned} C_{\nu}^{(1)}(\mathbf{r}, t) &= -v_T^2 \int d^2 \hat{\sigma} \hat{\sigma}_{\nu} g_2(\mathbf{r}, \mathbf{r} + \hat{\sigma} | n) n(\mathbf{r}, t) n(\mathbf{r} + \hat{\sigma}, t) \\ &\quad \times \left\{ 1 - \frac{2}{v_T \sqrt{\pi}} \sum_{\nu} \hat{\sigma}_{\nu} [u_{\nu}(\mathbf{r} + \hat{\sigma}, t) - u_{\nu}(\mathbf{r}, t)] \right. \\ &\quad \left. + \frac{k_B [T(\mathbf{r} + \hat{\sigma}, t) - T(\mathbf{r}, t)]}{2m v_T^2} \right\} \end{aligned} \quad (12)$$

The next  $C^{(2)}$  term, governing energy transport, can be derived explicitly and reads

$$\begin{aligned} C^{(2)}(\mathbf{r}, t) &= v_T^2 \sigma^2 \int d^2 \hat{\sigma} g_2(\mathbf{r}, \mathbf{r} + \hat{\sigma} | n) n(\mathbf{r}, t) n(\mathbf{r} + \hat{\sigma}, t) \\ &\quad \times \left\{ - \sum_{\nu=1}^3 \hat{\sigma}_{\nu} \frac{[u_{\nu}(\mathbf{r} + \hat{\sigma}, t) - u_{\nu}(\mathbf{r}, t)]}{2} \right. \\ &\quad \left. + \frac{1}{\sqrt{\pi}} \frac{k_B [T(\mathbf{r} + \hat{\sigma}, t) - T(\mathbf{r}, t)]}{m v_T} \right\} \end{aligned} \quad (13)$$

Having, now, an explicit representation for  $C_\nu^{(1)}$  and  $C^{(2)}$  in terms of the local values of the five hydrodynamic fields we can solve by iteration the equation of evolution for  $f(\mathbf{r}, \mathbf{v}, t)$ , compute the new values of the fields and proceed. Notice that in order to extract the momentum flux and the heat flux one has to use formulae (4) and (5)

The inclusion of energy transport in LB is, however, conditioned by the stability of the numerical method. In fact, it is well known that non-isothermal LB schemes suffer from rather severe instabilities already at the level of ideal fluids [12]. In the following, we have thus considered the regime in which thermal gradients are small, i.e. by taking  $T = const$  in eqs. (12) and (13).

The radial distribution function appearing in (12) is constructed according to the following prescription, dating back to Fischer and Methfessel [23]. At first, one defines a coarse-grained density  $\bar{n}(\mathbf{r}, t)$  via a uniform smearing over a sphere of radius  $\sigma/2$ , and the coarse-grained packing fraction is  $\bar{\eta}(\mathbf{r}, t) = \pi\sigma^3\bar{n}(\mathbf{r}, t)/6$ . Next, the equilibrium radial distribution function,  $g_2(\mathbf{r}, \mathbf{r} + \boldsymbol{\sigma}|n)$ , is replaced by the following approximation [24]  $g_2(\mathbf{r}, \mathbf{r} + \boldsymbol{\sigma}) \simeq [(1 - \bar{\eta}(\mathbf{r} + \boldsymbol{\sigma}/2)/2 + \bar{\eta}^2(\mathbf{r} + \boldsymbol{\sigma}/2)/4)/[1 - \bar{\eta}(\mathbf{r} + \boldsymbol{\sigma}/2)]^3$ .

In order to evaluate the surface integrals we choose  $\sigma$  to be an even multiple of the lattice spacing and employ a 18-point quadrature over a spherical surface [25]. With this choice, the elements arising from  $g_2$  and the hydrodynamic moments are taken from 6 on-lattice quadrature points while the elements arising from the remaining 12 off-lattice points are constructed via a linear interpolation from the surrounding on-lattice elements.

We have found that this approximation for the pair correlation function gives excellent results when the coupling between density and current in eqs. (12) and (13) is absent, corresponding to a dynamical DFT treatment. However, when the coupling is active, correlations are spuriously enhanced even for the static case. This problem can be traced back to the well-known compressibility error intrinsic to the LB discretization [12], i.e. the fluid current is not rigorously divergence free in absence of external forcing. In order to alleviate such a problem, we have introduced in the density-current convolution of eq.(12) a space-dependent regularizing factor  $(1 - \exp(-|r - r_w|/\sigma))$ , where  $r_w$  is the position of the wall. An alternative to this intervention could be the use of an Hermite basis set with higher components than the one associated to the D3Q19 lattice scheme.

*Numerical validation.* As a first test of our scheme we have determined the shear viscosity of a uniform system by performing a linear analysis of the equations of motions for the hydrodynamic fields (to be published elsewhere), obtained from eq. (3) and eq. (12). It can be shown that the present theory gives a shear viscosity identical to that predicted by a method proposed long ago by Longuet-Higgins and Pople (LHP) [26]. In fig.1 we display the numerical results together with the predictions of the LHP theory and the Enskog theory which, as it is well known,

gives a value of  $\eta$  larger than that obtained from the LHP route [27].

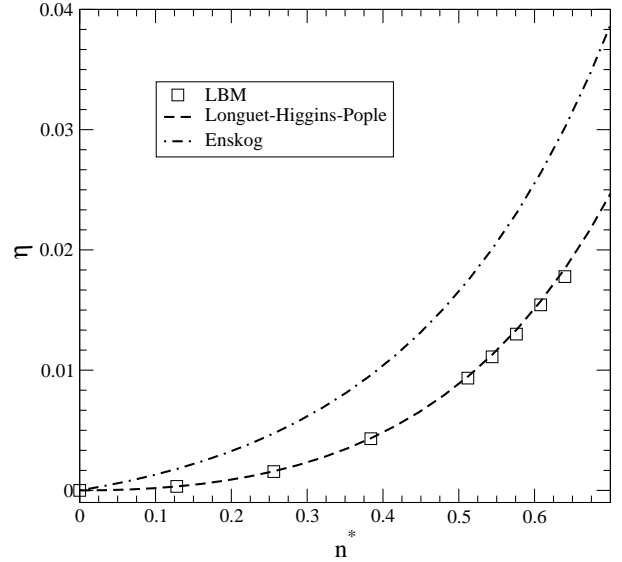


Fig. 1: Collisional contribution to the excess part of the bulk shear viscosity obtained through: the Longuet-Higgins and Pople theory ( $\eta = \frac{4}{15}\sqrt{k_B T m} g_2(\sigma)(n_{bulk}^*)^2 \sigma^4$ ) [26] (dashed line), Enskog theory ( $\eta = \frac{5}{16\sigma^2}\sqrt{\frac{k_B T m}{\pi}}(0.8\frac{2\pi}{3}n_{bulk}^* + 0.7737g_2(\sigma)\frac{4\pi^2}{9}(n_{bulk}^*)^2)$ ) [27] (dot-dashed line), and numerical data obtained from the time decay of a transverse velocity perturbation (squares).

Next, we have considered the equilibrium structure of the hard-sphere fluid. No-slip boundary conditions are enforced on the fluid velocity at the wall via a bounce-back method [12]. The corresponding density profiles are reported in fig.2 at various values of the average density together with a comparison with the results of equilibrium Monte Carlo simulations. Clearly, the fluid is more inhomogeneous at higher densities and displays oscillatory behavior in the regions adjacent to the walls. These oscillations become less evident toward the center of the slit. As compared to the exact Monte Carlo solution, the LB data provide slightly less correlated profiles. It is worth mentioning that the LB solution is achieved with a CPU effort about 30 times smaller than needed to generate converged Monte Carlo data.

By considering the fluid flow induced by the presence of a uniform field,  $\mathbf{F}_e$ , parallel to the walls of the slit, the streaming velocity profiles corresponding to different values of the bulk density are shown in fig.3. We notice that as the bulk density increases also the current profiles display a non-monotonic structure close to the walls. In addition, the average streaming velocity decreases as the density increases as a consequence of mutual steric hindrance among particles.

Finally, in fig. 4 we have considered the dependence of the streaming profiles on the width of the slit and, for the sake of comparison, displayed the results against

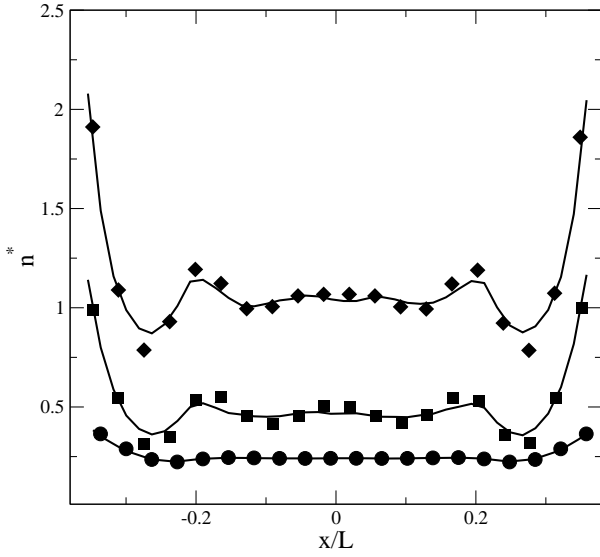


Fig. 2: Static density profiles in a slit of width  $L/\sigma = 5$  at  $n_{bulk}^* = 0.256$  (lower curve),  $n_{bulk}^* = 0.512$  (mid curve) and  $n_{bulk}^* = 0.609$  (upper curve) as compared to Monte Carlo simulations. The data at higher density have been shifted by an arbitrary value.

the parabolic velocity profiles *à la* Poiseuille, predicted by the Navier-Stokes theory. Interestingly, the central region does not exhibit significant deviations from the quadratic behavior of the classical theory, while a non monotonic profile next to the walls becomes more pronounced for the narrower systems [28].

**Conclusions.** – In summary, we have presented a theoretical analysis and computational scheme which bridge hydrodynamics with microscopic structural theories of fluids. We stress that the present method has been derived starting from a microscopic model of the fluid and, unlike the very popular and successful Shan-Chen method, truly represents a bottom-up approach to the description of fluid transport.

In order to simulate microscopic flows, however, the LB method should be employed with care. In nanofluidic conditions, the ratio between the mean free path and the characteristic length (the Knudsen number) can be rather high. On the contrary, the LB method in the current implementation (with the D3Q19 finite Hermite basis) is designed to deal with low-Knudsen conditions, namely in the range of validity of the Navier-Stokes equations. Recently, however, a generalization of the numerical method to deal with high-Knudsen conditions has been proposed [29], that basically extends the Hermite basis up to the third order and removes off-basis contributions. We believe that such an extension, together with the kinetic approach described in this paper, would yield a relevant step forward in the study of out-of-equilibrium microscopic flows.

A straightforward generalization of the present work can accommodate attractive forces, which are essential ingredients in order to describe multi-phase behavior. A detailed

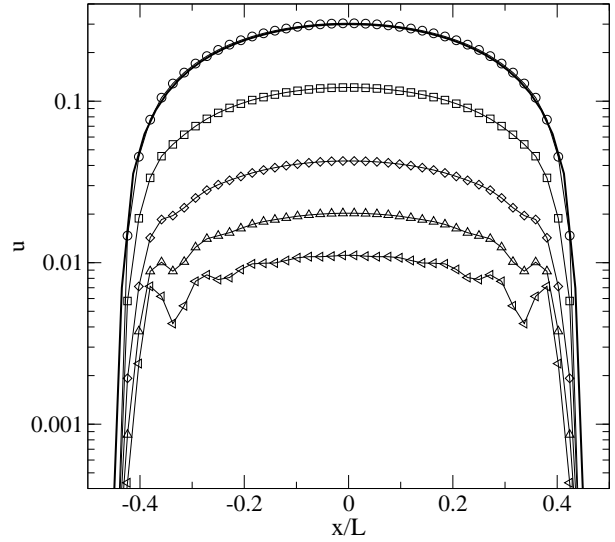


Fig. 3: Poiseuille velocities under the influence of the external field  $F_e/\sigma^3 = 2.410^{-6}$  for a slit of width  $L/\sigma = 10$  at various bulk densities:  $n_{bulk}^* = 0.064$  (circles), 0.128 (squares), 0.256 (diamonds), 0.384 (triangles up), and 0.512 (triangles left).

description of the calculations reported in the present communication will be published elsewhere.

**Acknowledgments.** – U.M.B.M. acknowledges the support of the Project Complex Systems and Many-Body Problems Cofin-MIUR 2005 prot. 2005027808.

## REFERENCES

- [1] H. LÖWEN, J. Phys.: Condens. Matter 14, 11897 (2002).
- [2] T.M. SQUIRES AND S.R. QUAKE, Rev. Mod. Phys. 77, 977 (2005).
- [3] R. EVANS, Adv. Phys., 28, 143 (1979)
- [4] U. MARINI BETTOLO MARCONI AND P. TARAZONA, J. Chem. Phys. 110, 8032 (1999).
- [5] A. SANTOS, J. M. MONTANERO, J. W. DUFTY, AND J. J. BREY, Phys. Rev. E 57, 1644 (1998).
- [6] N. S. MARTYS AND X. SHAN AND H. CHEN, Phys. Rev. E 58, 6855 (1998)
- [7] X. HE AND G.D. DOOLEN, J. S
- [8] H.T. DAVIS, J. Chem. Phys. 86, 1474(1987)at. Phys. 107, 309 (2002).
- [9] Z. GUO, T. S. ZHAO AND Y. SHI, Phys. Rev. E 71, 035301(R) (2005)
- [10] R. BENZI, S. SUCCI AND M. VERGASSOLA, Phys. Rep. 222, 3 (1992).
- [11] F. HIGUERA, S. SUCCI AND R. BENZI, Europhys. Lett. 9, 345 (1989).
- [12] S. SUCCI, *The lattice Boltzmann equation for fluid dynamics and beyond*, 1th edition (Oxford University Press, 2001)
- [13] G.G. MCNAMARA AND G. ZANETTI, Phys. Rev. Lett. 61, 2332 (1988).
- [14] X. SHAN AND H. CHEN, Phys. Rev. E 49, 2941 (1994).
- [15] R. BENZI, L. BIFERALE, M. SBRAGAGLIA, S. SUCCI, AND F. TOSCHI, Phys. Rev. E 74, 021509 (2006)

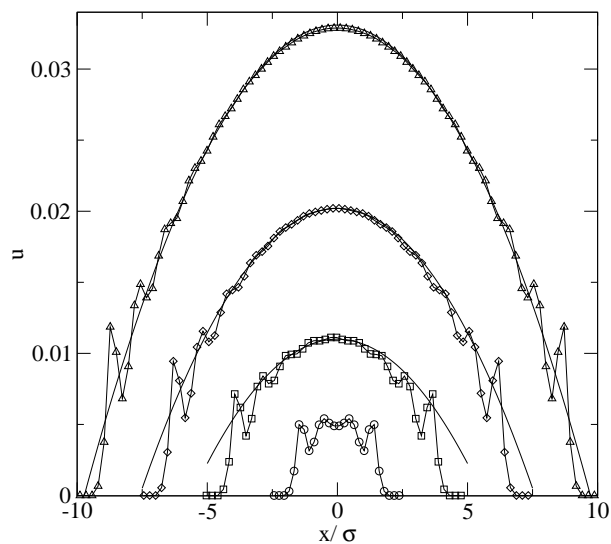


Fig. 4: Poiseuille velocities under the same forcing of fig. 3 for  $n_{bulk}^* = 0.512$  at various slit widths:  $L = 20\sigma$  (triangles),  $15\sigma$  (diamonds),  $10\sigma$  (squares) and  $5\sigma$  (circles).

- [16] M. SWIFT, W. OSBORNE AND J. YEOMANS, Phys. Rev. Lett. 75, 830 (1995).
- [17] N.S. MARTYS, Intl. J. Mod. Phys. 10, 1367 (1999).
- [18] P. TARAZONA AND U. MARINI BETTOLO MARCONI, J. Chem. Phys. 124, 164901 (2006).
- [19] U. MARINI BETTOLO MARCONI AND S. MELCHIONNA, J. Chem. Phys. 126, 184109 (2007).
- [20] H. VAN BELJEREN AND M.H. ERNST, Physica (Utrecht) 68, 437 (1973) and 70, 225 (1973).
- [21] X. SHAN AND X. HE, Phys. Rev. Lett. 80, 65 (1998)
- [22] X. HE AND L.-S. LUO, Phys. Rev. E 55, R6333 (1997)
- [23] J. FISCHER AND M. METHFESSEL, Phys. Rev. A 22, 2836 (1980)
- [24] J.-P. HANSEN AND I.R. McDONALD, *Theory of Simple Liquids*, 3rd Edition (Academic Press, London, 2006).
- [25] M. ABRAMOWITZ AND I. A. STEGUN, *Handbook of Mathematical Functions*, 9th edition (Dover, New York, 1972)
- [26] H.C. LONGUET-HIGGINS AND J.A. POPLE, J.Chem.Phys. 25, 884 (1956)
- [27] H. SIGURGEIRSSON AND D. M. HEYES, Mol. Phys. 101, 469 (2003)
- [28] K.P. TRAVIS AND K. E. GUBBINS, J. Chem. Phys. 112, 1984 (2000)
- [29] X. SHAN, X. YUAN AND H. CHEN, J. Fluid. Mech. 550, 413 (2006)